INSTITUTE OF PHYSICS PUBLISHING JOURNAL OF PHYSICS B: ATOMIC, MOLECULAR AND OPTICAL PHYSICS

J. Phys. B: At. Mol. Opt. Phys. **38** (2005) 2371–2384 doi:10.1088/0953-4075/38/14/004

Differential and integrated cross sections for the elastic electron scattering by calcium atom

S Milisavljević[1], D Šević[1], R K Chauhan[2], V Pejčev[1,3], D M Filipović[1,4], R Srivastava[2] and B P Marinković[1]

[1] Institute of Physics, Belgrade, PO Box 68, 11080 Belgrade, Serbia and Montenegro
[2] Department of Physics, Indian Institute of Technology, Roorkee 247667, India
[3] Faculty of Natural Sciences, University of Kragujevac, Serbia and Montenegro
[4] Faculty of Physics, University of Belgrade, PO Box 368, 11001 Belgrade, Serbia and Montenegro

E-mail: bratislav.marinkovic@phy.bg.ac.yu

Received 10 February 2005, in final form 25 May 2005
Published 20 June 2005
Online at stacks.iop.org/JPhysB/38/2371

Abstract

The experimental and theoretical studies of elastic electron scattering by calcium atom have been made. The experimental investigation was carried out using a crossed electron-atom beam technique. The measurements were performed at electron-impact energies (E_0) of 10, 20, 40, 60 and 100 eV and for a range of scattering angles (θ) from 10° up to 150°. The absolute differential cross sections (DCSs) have been obtained from the elastic-to-inelastic (the resonant 4^1P^0 state) intensity ratio at $\theta = 10°$ at each E_0. Calculations have been performed in the optical potential approximation for the same E_0 and θ between 0° and 180°. Results for DCSs and integrated (integral, momentum transfer and viscosity) cross sections are presented and compared with those predicted by existing calculations.

(Some figures in this article are in colour only in the electronic version)

1. Introduction

In recent years, there have been numerous studies of elastic electron scattering by metal atoms. Although a considerable number of papers have been devoted to these processes, they still attract a lot of attention from both the experimental and theoretical fields. Differential cross sections (DCSs) for electron scattering are very important for explanation and understanding of electron interaction with different atoms and molecules and for determining dynamics of the collision processes.

In our previous paper [1], we reported results on electron-impact excitation of the 4^1P^0 state of calcium atom. In order to complete our study of electron collision with calcium

atom, we performed elastic DCSs measurements in the intermediate electron-impact region from 10 to 100 eV and the scattering angle range from 10° to 150°. Calculations have been carried out within optical potential approximation for the same incident electron energies. Here we present our DCS results as well as calculated integral (Q_I), momentum transfer (Q_M) and viscosity (Q_V) cross sections. Elastic electron calcium scattering has been studied both experimentally and theoretically and several results are available regarding this process. The results of interest for our investigation reported by different authors [2–19] are summarized in table 1. Unfortunately, only a very limited amount of experimental and theoretical works have been done on the angle dependences of the DCSs. Even if we include results for integrated cross sections, there are only a few results reported of this scattering process in the energy range considered here. In the work by Gregory and Fink [2], based on solving the Dirac equation, the elastic electron calcium DCSs have been reported at energies varying from 100 eV to 2 keV but these calculations excluded the electron exchange and polarization effects. The other theoretical descriptions and calculations are mainly based on optical potential approximation in which the main problem is exact determination i.e. direct calculation of the optical potential of the system which is a complex, non-local, energy-dependent non-spherically symmetric potential. Therefore, several approximations were performed where optical potential was represented by different potentials. Khare *et al* [5] used the optical model calculation for elastic electron and positron scattering by calcium atom. They obtained differential and integral elastic cross sections, the critical points, the direct and spin-flip scattering amplitudes (f and g) and spin polarization parameters $S(\theta)$, $T(\theta)$ and $U(\theta)$ in the energy range from 10 to 500 eV. The many-body problem was reduced to a one-body problem and optical potential of the system was represented by a spherically symmetric, localized and real potential which consists of static, exchange and polarization potentials. According to this, they performed results in the static-field (SF), static-field-polarization-exchange (SFPE) and static-field-polarization-exchange-spin-orbit (SFPESO) approximations. A calculation for the elastic scattering of slow electron has been carried out by Nikolić and Tančić [14]. They obtained DCS in the Hartree Fock and random phase approximation with exchange for polarization potential. The main motivation for work by Yuan [15] was to examine the influence of intra-atomic relativistic effects on electron spin polarization in the low-energy (0.01–20 eV) electron scattering. In order to study the importance of these effects, he used three different kinds of atomic wavefunctions: Dirac Fock (DF), quasirelativistic Hartree Fock (QRHF) and non-relativistic Hartree Fock (HF) for bounded electrons and obtained three sets of DCS and Q_I results. The momentum transfer cross sections were obtained using only DF atomic wavefunction. The study by Kelemen *et al* [16] was concerned with elastic and inelastic scattering in the energy range up to 200 eV. Using the complex optical potentials they calculated DCSs for elastic electron calcium scattering at energies below the inelastic threshold and integral elastic cross sections in the whole energy region up to 200 eV. Buckman and Clark [20] have summarized the extensive work done on observing resonance phenomena in electron-calcium scattering.

In the present work, we present results of investigations of the elastic electron scattering by Ca atom. In order to give complete set of data and make basis for further study of this elastic electron-calcium process, optical potential calculations have also been performed. The obtained results include DCSs and integrated cross sections. Experimental DCSs were extrapolated to 0° and 180° and numerically integrated to yield Q_I, Q_M and Q_V. We measured angular distribution of electrons elastically scattered by calcium atom for electron-impact energies of 10, 20, 40, 60 and 100 eV and within a scattering angle interval from 10° to 150° in steps of 10° except at 20 eV where the scattering intensities were recorded at each 2° from 70° up to 90°. Elastic scattering intensities below 10° were not recorded because of direct

Table 1. Summary of experimental and theoretical works on elastic electron calcium scattering.

Author	Theory/Experiment	Results	Parameters
Gregory and Fink [2]	Dirac equation	Angle-dependent DCS	$E_0 = (100–2000)$ eV $\theta = (0–178)^\circ$
Romanyuk *et al* [3]	Crossed beam electron trap	Total CS	$E_0 = (0–10)$ eV
Kurtz and Jordan [4]	SE, SEP	Partial (s, p, d, f) and integral elastic CS	$E_0 = (0–5)$ eV
Khare *et al* [5]	SF, SFPE, SFPESO	Angle-dependent DCS Integral elastic CS	$E_0 = (10–500)$ eV $\theta = (0–180)^\circ$
Amusia *et al* [6]	Dyson equation	Integral elastic CS	$E_0 < 5$ eV
Kazakov and Kristoforov [7]	Crossed beam 127° cylindrical analyser	Energy-dependent DCS	$E_0 = (0–7)$ eV $\theta = 90^\circ$
Kelemen *et al* [8]	OP	Integral elastic CS	$E_0 = (0–50)$ eV
Yuan and Zhang [9]	SE[a]	Partial (s, p, d) and integral elastic CS	$E_0 = (0.01–3)$ eV
Yuan and Zhang [10]	SE[b]	Partial (s, p, d) and integral elastic CS Energy-dependent DCS	$E_0 = (0.01–5)$ eV $\theta = 90^\circ$
Gribakin *et al* [11]	Dyson equation	Phase shift (p)	$E_0 < 1.3$ eV
Kelemen *et al* [12]	OP	Integral elastic CS	$E_0 = (0–40)$ eV
Gribakin *et al* [13]	Dyson equation	Phase shifts (s, p, d, f)	$E_0 < 3.5$ eV
Nikolić and Tančić [14]	Dyson equation	Angle-dependent DCS	$E_0 = 8.7$ eV $\theta = (0–180)^\circ$
Yuan [15]	DF, QRHF, HF	Integral elastic and momentum transfer CS Angle-dependent DCS	$E_0 = (0.01–20)$ eV $E_0 = (0.05–10)$ eV $\theta = (0–180)^\circ$
Kelemen *et al* [16]	OP	Angle-dependent DCS Energy-dependent DCS Partial (s, p, d, f) and integral elastic CS	$E_0 = (0.1–1.8)$ eV $\theta = (0–180)^\circ$ $\theta = (50, 54.7, 90)^\circ$ $E_0 = (0.1–200)$ eV
Dapor [17]	Dirac equation	Momentum transfer CS	$E_0 = (500–4000)$ eV
Yuan and Fritsche [18]	CC	Partial (s, p, d) and integral elastic CS	$E_0 = (0–4)$ eV
Remeta *et al* [19]	PW	Energy-dependent DCS	$E_0 = (0.1–1.8)$ eV

DCS: differential cross section, CS: cross section, SF: static-field approximation, SFPE: static-field-polarization-exchange approximation, SFPESO: static-field-polarization-exchange-spin-orbit approximation, OP: complex optical potential, SE: static exchange, SEP: static exchange plus polarization calculation, SE[a]: static exchange plus correlation-polarization potential, SE[b]: static exchange plus correlation-polarization potential (the screening, spin-polarization and relativistic effects are accounted), DF: Dirac Fock atomic wavefunction, QRHF: Cowan quasirelativistic Hartree Fock atomic wavefunction, HF: non-relativistic Hartree Fock atomic wavefunction, CC: close-coupling calculation using R-matrix method, PW: partial-wave expansion.

beam contribution. Our differential and integral cross sections are compared with existing calculations by Gregory and Fink [2], Khare *et al* [5], Yuan [15] and Kelemen *et al* [16].

2. Experimental technique and procedure

The measurements were conducted using perpendicularly crossed electron and atom beams. The experimental apparatus as well as experimental technique and procedure have been

described earlier [1, 21]. Therefore, we shall not describe them in detail and only a brief summary will be given.

The electrons from hairpin thermoelectron source pass through the systems of cylindrical electrostatic lenses made of gold-plated oxygen-free high conductivity copper and hemispherical electrostatic energy selector made of molybdenum (electron monochromator). A monoenergetic beam of electrons (full width at half maximum FWHM around 100 meV) from the monochromator was perpendicularly crossed by the atomic beam and elastically scattered electrons were analysed and detected as a function of scattering angle at fixed electron-impact energy E_0 by the hemispherical electron energy analyser and channel electron multiplier as a single-electron detector. The analyser can be positioned from -30° to 150° with respect to the incoming electron beam.

Calcium vapour beam was produced by heating oven crucible containing Ca metal (99.5% purity) by two separate heaters and was effused through a cylindrical channel (aspect ratio $\gamma = 0.075$) in the cap of the oven crucible. Working temperature was about 700–720 °C and background pressure was of the order of 10^{-5} Pa. The energy scale was calibrated by measuring the position of the feature in the elastic scattering attributed to the threshold energy of the 4^1P^0 excitation of calcium at 2.93 eV. The uncertainty of the energy scale is determined to be 100 meV, overall energy resolution of 160 meV and the angular resolution was estimated to be 1.5°.

Before each measurement an energy loss spectrum was obtained. The position of true zero scattering angle was determined from the symmetry of 4^1P^0 angular scattering distribution around 0° (from -10° to $+10^\circ$) for each E_0. An effective length correction factors [22] appropriate to our experimental conditions converted the measured elastic scattering signals to relative DCSs. The absolute DCS values were obtained from the measurements of elastic-to-inelastic intensity ratios and using the absolute DCS of the resonant 4^1P^0 state at $\theta = 10^\circ$. The intensity ratios have been measured in two ways, with two different tuning of the analyser. Once we focused the elastic signal and then the 4^1P^0 and final ratio values have been obtained as geometrical mean of two different ratio measurements. We performed this procedure for each E_0. Absolute DCSs were extrapolated to 0° and 180° upon present calculations in static-exchange-polarization approximation and then integrated to obtain integral, momentum transfer and viscosity cross sections (equations (3)–(5) in [1]).

3. Theoretical calculation

To theoretically calculate different cross sections for the elastic scattering of electrons from calcium atoms, we obtain the scattering amplitude by conventional method of partial wave analysis and solve the Schrödinger wave equation using suitable optical potential [23]. The optical potential consists of the sum of the static ($V_{\rm stat}$), exchange ($V_{\rm ex}$) and polarization ($V_{\rm pol}$) potentials [5, 24]:

$$V_{\rm opt}(r) = V_{\rm stat}(r) + V_{\rm pol}(r) + V_{\rm ex}(r). \tag{1}$$

Our choice of these various potentials namely, the exchange and polarization potentials is slightly different than those adopted in [5] for studying the elastic scattering of electrons from calcium atoms. The static potential $V_{\rm stat}$ has been obtained as in [5] by using accurate (HF) wave-function of the ground state of calcium atom [25]. The exchange potential $V_{\rm ex}$ is non-local but it is usually taken for the sake of simplicity to be local and energy dependent. Majority of earlier calculations including Khare *et al*'s [5] have used the local exchange potential given by Furness and McCarthy [26], which is especially suitable for high electron-impact energies. However, later Gianturco and Scialla [27] modified this exchange potential

so that it is also applicable to low energies and we have used the same exchange potential in our present calculation. For the polarization potential, the following form has been taken which is widely used and tested to produce good results:

$$V_{\mathrm{pol}}(r) = -\frac{\alpha_{\mathrm{d}} r^2}{2(r^2 + d^2)^3}, \tag{2}$$

where $\alpha_{\mathrm{d}} = 168.71$ is static dipole polarizabilty of the calcium atom in its ground the $4^1\mathrm{S}_0$ state [28]. The parameter d is taken from the paper of Mittleman and Watson [29] and is given by

$$d = \left(\tfrac{1}{2}\alpha_{\mathrm{d}}\beta^2 Z^{-\frac{1}{3}}\right)^{\frac{1}{4}}. \tag{3}$$

Here β is parameter dependent on the incident electron energy and is chosen to provide best fit to the experimental differential cross section results. In our calculation, we have chosen β such that it provides best shape fitting to the experimental differential cross section data at a particular energy. Our values of β vary in the range of 0.319–0.639 for the incident electron energy range from 10 to 100 eV. These β values correspond to the cut-off radius d in the range of 2.20–3.11 which seem quite consistent with the values of cut-off radius taken in the similar polarization potential used in the recent study of elastic electron scattering from Sr and Ba atoms [30]. In some of the calculations as in [5], an additional quadrupole term is also added to the dipole term i.e. the expression of polarization potential given in equation (2). This is to take account of static quadrupole polarization, which varies asymptotically as r^{-6}. However, we found through our present and earlier calculations [24] that by adding this term the effect is only at low energies ($\leqslant$20 eV) and the agreement with experiment worsens while there is negligible effect at high energies. This behaviour at low energies suggests that further higher terms should also be included for proper cancellation.

4. Results and discussion

Elastic electron scattering by calcium atom has been studied experimentally and theoretically. We have measured angular distribution of electrons elastically scattered by calcium atom at 10, 20, 40, 60 and 100 eV electron-impact energies from 0° to 150° in 10° increments. At 20 eV and θ from 70° to 90° scattered electron intensities have been measured in steps of 2°. The calculations have been performed in the static, static-exchange and static-exchange-polarization approximations.

We have measured elastic-to-inelastic (the resonant $4^1\mathrm{P}^0$ state) intensity ratios and using the absolute DCS of the resonant $4^1\mathrm{P}^0$ state at $\theta = 10°$, we have obtained the factors (table 2), which were used for putting relative cross sections on an absolute scale. The structure and change of DCS curves are shown in figure 1 (see tables 3 and 4). The shapes of the elastic experimental DCS curves change as a function of electron-impact energy as shown in figure 1(a). At 10 eV there are three minima, at 30°, 70° and 120°. The second minimum becomes deeper at 20 eV (84°) while at 40 and 60 eV the second and the third minima are of equal depth. The first minimum at lower scattering angle slowly transforms into a shoulder around 35° at 60 eV. At small scattering angles, DCS curve for 100 eV is rather flat and generally has only two minima, one at 70° and the other at 130°. Generally, the calculated DCSs (figure 1(b)) have the similar shapes as the experimental ones. At 10 eV there are also three minima, at 44°, 89° and 134°. As the energy increases, the second moves towards smaller scattering angles, from 80° at 20 eV, 70° at 40 eV, 65° at 60 eV to 61° at 100 eV. The first minimum disappears and the third becomes more pronounced. In figure 1(b) DCS results in static, static-exchange and static-exchange-polarization approximations at 40, 60

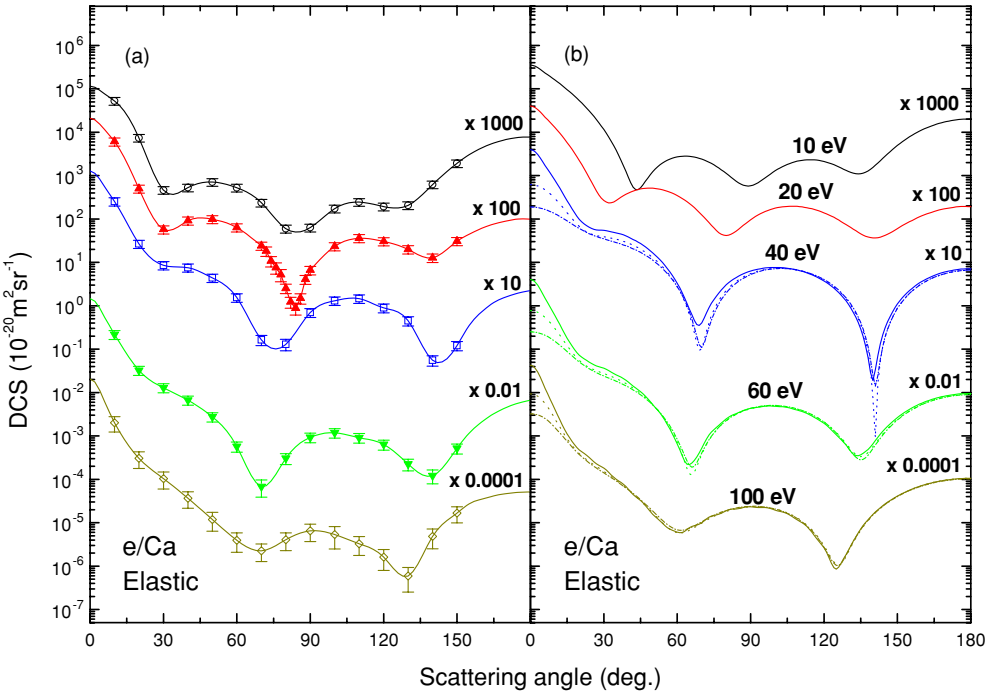

Figure 1. Differential cross sections for elastic electron scattering by Ca atom. (a) Experiment: ○, 10 eV; ▲, 20 eV; □, 40 eV; ▼, 60 eV; ◇, 100 eV electron-impact energy. The curves are multiplied by the indicated factor. (b) Calculations: ——, static-exchange-polarization approximation; . . . , static-exchange approximation; – · – ·, static approximation.

Table 2. Elastic-to-inelastic (the resonant 4^1P^0 state) intensity ratio at $\theta = 10^\circ$ with absolute errors indicated.

Energy (eV)				
10	20	40	60	100
1.00 ± 0.08	1.2 ± 0.2	0.8 ± 0.1	1.2 ± 0.2	2.4 ±0.6

and 100 eV are also shown. As one can see, positions of the minima corresponding to all these approximations are in good agreement. It has been found that at 40 eV, DCSs in static and static-exchange approximations have deeper minima from that in static-exchange-polarization approximation. However, as the energy increases, all the approximations come closer and at 100 eV they give nearly the same results except at small scattering angles.

No other experimental data are available for comparison. A comparison of the present experimental and calculated DCSs is presented in figures 2(a) and (b) for 10 and 20 eV respectively. At the lowest electron-impact energy (10 eV), the static and static-exchange calculations are similar in shapes except static DCS, which shows more pronounced minimum at 120°. However, the behaviour of static-exchange-polarization DCS is completely different and minima are displaced from those of DCSs in previous approximations. Also, it could be seen that adding exchange and polarization effects leads to the rising of the absolute DCS values. Experiment gives smaller DCSs and there is less agreement with theory. In order

Table 3. Differential cross sections and absolute errors (in units of 10^{-20} m^2 sr^{-1}) for elastic electron scattering by Ca atom. The last three lines are determined integral (Q_I), momentum transfer (Q_M) and viscosity (Q_V) cross sections in units of 10^{-20} m^2 with absolute errors indicated.

	Energy (eV)				
Angle (°)	10	20	40	60	100
10	52.6 ± 10.5	60.8 ± 14.1	25.3 ± 5.4	21.8 ± 5.0	20.1 ± 7.8
20	7.39 ± 1.47	4.98 ± 1.15	2.67 ± 0.57	3.25 ± 0.76	3.05 ± 1.26
30	0.464 ± 0.093	0.575 ± 0.133	0.857 ± 0.184	1.29 ± 0.30	1.04 ± 0.44
40	0.529 ± 0.105	0.915 ± 0.212	0.756 ± 0.163	0.668 ± 0.158	0.365 ± 0.149
50	0.711 ± 0.142	0.986 ± 0.228	0.438 ± 0.095	0.276 ± 0.067	0.119 ± 0.055
60	0.525 ± 0.105	0.639 ± 0.148	0.155 ± 0.034	0.0575 ± 0.0152	0.0396 ± 0.0187
70	0.237 ± 0.047	0.241 ± 0.056	0.0164 ± 0.0043	0.00680 ± 0.00290	0.0226 ± 0.0098
72		0.183 ± 0.048			
74		0.107 ± 0.030			
76		0.0754 ± 0.0228			
78		0.0522 ± 0.0172			
80	0.0596 ± 0.0122	0.0253 ± 0.0066	0.0130 ± 0.0038	0.0305 ± 0.0086	0.0408 ± 0.0179
82		0.0122 ± 0.0036			
84		0.00875 ± 0.00279			
86		0.0150 ± 0.0043			
88		0.0406 ± 0.0103			
90	0.0633 ± 0.0129	0.0661 ± 0.0161	0.0701 ± 0.0161	0.0929 ± 0.0232	0.0649 ± 0.0282
100	0.173 ± 0.035	0.234 ± 0.055	0.131 ± 0.029	0.118 ± 0.029	0.0533 ± 0.0285
110	0.246 ± 0.049	0.360 ± 0.084	0.146 ± 0.032	0.0914 ± 0.0229	0.0329 ± 0.0152
120	0.193 ± 0.039	0.305 ± 0.071	0.0894 ± 0.0203	0.0636 ± 0.0164	0.0161 ± 0.0081
130	0.206 ± 0.041	0.199 ± 0.047	0.0449 ± 0.0108	0.0225 ± 0.0068	0.00593 ± 0.00340
140	0.623 ± 0.124	0.127 ± 0.030	0.00556 ± 0.00150	0.0121 ± 0.0043	0.0484 ± 0.0232
150	1.91 ± 0.38	0.309 ± 0.072	0.0121 ± 0.0029	0.0520 ± 0.0135	0.167 ± 0.067
Q_I	22.1 ± 9.5	22.3 ± 8.7	10.5 ± 4.1	10.4 ± 4.5	10.5 ± 5.9
Q_M	11.0 ± 3.8	4.07 ± 1.53	1.31 ± 0.48	1.39 ± 0.59	1.27 ± 0.65
Q_V	3.17 ± 1.21	3.08 ± 1.22	1.38 ± 0.52	1.23 ± 0.58	0.87 ± 0.47

to make a comparison, the DCS results by Yuan [15] are also shown in this figure. It is worthwhile to mention that the same results are obtained in all three sets of calculations (DF, QRHF and HF). The DCS curves cannot be distinguished from each other, so we present here only results of the first set obtained with DF atomic wavefunction. It is obvious that there is a good agreement considering absolute values between experimentally obtained DCS and DF results. The calculation also predicts three minima but the position of the second minimum is quite different from that of the experimental DCS curve (it is moved towards smaller scattering angles). It is interesting that position of the third minimum (at approximately 120°) is very close to that in the experimental curve and the magnitude is the same as in our static approximation. We also compare present calculations with those by Khare *et al* [5] obtained with SFPE approximation in the limited angular range from 25 to 125° (see inset in figure 2(a)) since both calculations give almost the same values at lower scattering angles. The difference in our calculation with that in [5] for larger scattering angles ($\theta > 90°$) may be due to both exchange plus polarization. We normalized experimental results to present calculations at 10° and presented them in the same inset. At 20 eV, the absolute experimental DCSs are still lower than theoretical DCSs, but the shapes of angular distribution are in better agreement with static-exchange-polarization calculations. In order to compare experimental and calculated

Table 4. Differential cross sections (in units of 10^{-20} m^2 sr^{-1}) for elastic electron scattering by Ca atom in static (s), static-exchange (s-e) and static-exchange-polarization (s-e-p) approximations. The last three lines are determined integral (Q_I), momentum transfer (Q_M) and viscosity (Q_V) cross sections in units of 10^{-20} m^2.

	Energy (eV)														
Angle	10			20			40			60			100		
(°)	s	s-e	s-e-p	s	s-e	s-e-p	s	s-e	s-e-p	s	s-e	s-e-p	s	s-e	s-e-p
0	1.39E+01	3.99E+01	3.53E+02	1.47E+01	4.19E+01	4.01E+02	1.90E+01	6.20E+01	3.98E+02	2.51E+01	7.76E+01	4.04E+02	3.24E+01	9.34E+01	4.28E+02
5	1.35E+01	3.70E+01	2.55E+02	1.41E+01	3.70E+01	2.55E+02	1.73E+01	5.11E+01	2.09E+02	2.22E+01	6.02E+01	1.89E+02	2.74E+01	6.51E+01	1.70E+02
10	1.22E+01	3.10E+01	1.60E+02	1.25E+01	2.69E+01	1.29E+02	1.32E+01	2.99E+01	7.88E+01	1.52E+01	3.01E+01	6.00E+01	1.57E+01	2.51E+01	4.14E+01
15	1.05E+01	2.32E+01	9.57E+01	1.04E+01	1.65E+01	5.77E+01	9.01E+00	1.40E+01	2.63E+01	8.83E+00	1.21E+01	1.80E+01	7.51E+00	8.60E+00	1.11E+01
20	8.42E+00	1.57E+01	5.34E+01	8.44E+00	9.46E+00	2.22E+01	6.02E+00	6.71E+00	9.83E+00	5.07E+00	5.49E+00	7.25E+00	3.74E+00	3.91E+00	4.78E+00
25	6.39E+00	9.73E+00	2.68E+01	6.79E+00	6.09E+00	7.08E+00	4.36E+00	4.48E+00	6.05E+00	3.28E+00	3.55E+00	4.67E+00	2.18E+00	2.35E+00	2.83E+00
30	4.60E+00	5.73E+00	1.15E+01	5.52E+00	4.98E+00	2.67E+00	3.48E+00	3.89E+00	5.47E+00	2.41E+00	2.75E+00	3.65E+00	1.41E+00	1.52E+00	1.82E+00
35	3.17E+00	3.41E+00	3.87E+00	4.53E+00	4.69E+00	2.65E+00	2.88E+00	3.44E+00	4.77E+00	1.83E+00	2.11E+00	2.56E+00	9.22E-01	9.61E-01	1.01E+00
40	2.16E+00	2.28E+00	9.22E-01	3.67E+00	4.39E+00	3.95E+00	2.30E+00	2.79E+00	3.86E+00	1.34E+00	1.49E+00	1.74E+00	5.77E-01	5.74E-01	5.94E-01
45	1.53E+00	1.85E+00	5.26E-01	2.87E+00	3.82E+00	4.94E+00	1.70E+00	2.02E+00	2.73E+00	8.90E-01	9.50E-01	1.05E+00	3.39E-01	3.22E-01	3.25E-01
50	1.23E+00	1.77E+00	1.23E+00	2.13E+00	3.02E+00	5.13E+00	1.12E+00	1.28E+00	1.65E+00	5.19E-01	5.27E-01	5.29E-01	1.87E-01	1.69E-01	1.56E-01
55	1.17E+00	1.84E+00	2.12E+00	1.47E+00	2.16E+00	4.53E+00	6.33E-01	6.87E-01	8.50E-01	2.49E-01	2.37E-01	2.29E-01	1.01E-01	8.74E-02	8.55E-02
60	1.27E+00	1.96E+00	2.70E+00	9.38E-01	1.39E+00	3.46E+00	2.77E-01	2.79E-01	3.30E-01	8.44E-02	7.18E-02	6.57E-02	6.86E-02	5.90E-02	6.10E-02
65	1.44E+00	2.07E+00	2.78E+00	5.56E-01	8.20E-01	2.28E+00	7.20E-02	6.20E-02	8.34E-02	2.10E-02	1.35E-02	2.18E-02	7.47E-02	6.70E-02	7.66E-02
70	1.63E+00	2.17E+00	2.39E+00	3.33E-01	4.70E-01	1.24E+00	1.08E-02	1.03E-02	4.03E-02	4.03E-02	3.74E-02	5.24E-02	1.06E-01	9.86E-02	1.00E-01
75	1.76E+00	2.21E+00	1.77E+00	2.51E-01	3.25E-01	6.21E-01	6.55E-02	8.05E-02	1.39E-01	1.18E-01	1.17E-01	1.40E-01	1.48E-01	1.41E-01	1.48E-01
80	1.81E+00	2.19E+00	1.13E+00	2.76E-01	3.33E-01	4.17E-01	1.97E-01	2.24E-01	3.04E-01	2.26E-01	2.24E-01	2.47E-01	1.91E-01	1.83E-01	1.90E-01
85	1.75E+00	2.08E+00	6.85E-01	3.62E-01	4.31E-01	5.79E-01	3.64E-01	3.95E-01	4.78E-01	3.39E-01	3.34E-01	3.45E-01	2.24E-01	2.17E-01	2.11E-01
90	1.58E+00	1.87E+00	5.82E-01	4.67E-01	5.57E-01	9.61E-01	5.25E-01	5.54E-01	6.33E-01	4.33E-01	4.25E-01	4.35E-01	2.39E-01	2.34E-01	2.34E-01
95	1.31E+00	1.58E+00	8.15E-01	5.53E-01	6.63E-01	1.41E+00	6.49E-01	6.71E-01	7.31E-01	4.91E-01	4.82E-01	4.80E-01	2.34E-01	2.31E-01	2.24E-01
100	9.74E-01	1.21E+00	1.29E+00	5.97E-01	7.19E-01	1.78E+00	7.16E-01	7.27E-01	7.64E-01	5.05E-01	4.97E-01	4.84E-01	2.08E-01	2.08E-01	1.96E-01
105	6.23E-01	8.21E-01	1.81E+00	5.90E-01	7.15E-01	1.95E+00	7.16E-01	7.19E-01	7.36E-01	4.75E-01	4.68E-01	4.55E-01	1.66E-01	1.68E-01	1.62E-01
110	3.09E-01	4.64E-01	2.21E+00	5.39E-01	6.58E-01	1.93E+00	6.54E-01	6.49E-01	6.48E-01	4.06E-01	4.02E-01	3.81E-01	1.16E-01	1.19E-01	1.08E-01
115	8.62E-02	2.04E-01	2.32E+00	4.64E-01	5.71E-01	1.72E+00	5.43E-01	5.33E-01	5.20E-01	3.11E-01	3.11E-01	2.90E-01	6.58E-02	6.94E-02	6.07E-02
120	6.11E-03	1.04E-01	2.11E+00	3.93E-01	4.83E-01	1.38E+00	4.02E-01	3.92E-01	3.74E-01	2.09E-01	2.11E-01	1.96E-01	2.73E-02	2.97E-02	2.64E-02

125	1.09E-01	2.15E-01	1.69E+00	3.55E-01	4.23E-01	1.02E+00	2.57E-01	2.48E-01	2.28E-01	1.17E-01	1.21E-01	1.07E-01	1.04E-02	1.09E-02	8.52E-03
130	4.18E-01	5.70E-01	1.25E+00	3.78E-01	4.21E-01	6.87E-01	1.30E-01	1.23E-01	1.08E-01	5.25E-02	5.73E-02	5.20E-02	2.28E-02	2.15E-02	2.34E-02
135	9.38E-01	1.18E+00	1.10E+00	4.82E-01	4.95E-01	4.56E-01	4.09E-02	3.67E-02	2.93E-02	2.81E-02	3.34E-02	3.70E-02	6.97E-02	6.73E-02	7.21E-02
140	1.65E+00	2.03E+00	1.55E+00	6.74E-01	6.53E-01	3.67E-01	2.48E-03	7.23E-04	1.90E-03	5.13E-02	5.69E-02	6.58E-02	1.52E-01	1.50E-01	1.56E-01
145	2.52E+00	3.07E+00	2.81E+00	9.52E-01	8.90E-01	4.21E-01	1.92E-02	1.92E-02	3.12E-02	1.22E-01	1.28E-01	1.48E-01	2.65E-01	2.66E-01	2.72E-01
150	3.49E+00	4.24E+00	4.96E+00	1.30E+00	1.19E+00	6.02E-01	8.68E-02	8.79E-02	1.10E-01	2.35E-01	2.41E-01	2.67E-01	4.02E-01	4.07E-01	4.13E-01
155	4.50E+00	5.46E+00	7.87E+00	1.68E+00	1.53E+00	8.67E-01	1.94E-01	1.95E-01	2.26E-01	3.74E-01	3.83E-01	4.13E-01	5.53E-01	5.64E-01	5.67E-01
160	5.46E+00	6.62E+00	1.13E+01	2.07E+00	1.87E+00	1.19E+00	3.23E-01	3.23E-01	3.64E-01	5.29E-01	5.38E-01	5.73E-01	7.00E-01	7.18E-01	7.20E-01
165	6.30E+00	7.65E+00	1.47E+01	2.43E+00	2.19E+00	1.49E+00	4.51E-01	4.51E-01	4.98E-01	6.72E-01	6.83E-01	7.22E-01	8.41E-01	8.63E-01	8.58E-01
170	6.96E+00	8.45E+00	1.76E+01	2.72E+00	2.44E+00	1.74E+00	5.62E-01	5.61E-01	6.12E-01	7.91E-01	8.03E-01	8.43E-01	9.41E-01	9.70E-01	9.67E-01
175	7.37E+00	8.96E+00	1.96E+01	2.90E+00	2.60E+00	1.94E+00	6.36E-01	6.35E-01	6.92E-01	8.69E-01	8.84E-01	9.28E-01	1.01E+00	1.04E+00	1.04E+00
180	7.52E+00	9.14E+00	2.02E+01	2.96E+00	2.66E+00	1.92E+00	6.62E-01	6.61E-01	7.11E-01	8.99E-01	9.11E-01	9.47E-01	1.02E+00	1.06E+00	1.06E+00
Q_{I}	2.56E+01	3.75E+01	8.98E+01	1.97E+01	2.51E+01	6.16E+01	1.29E+01	1.78E+01	3.62E+01	1.05E+01	1.48E+01	2.72E+01	8.14E+00	1.13E+01	2.02E+01
Q_{M}	2.11E+01	2.65E+01	3.95E+01	1.07E+01	1.17E+01	1.77E+01	5.16E+00	5.42E+00	6.30E+00	4.04E+00	4.14E+00	4.42E+00	2.91E+00	2.96E+00	3.03E+00
Q_{V}	1.11E+01	1.45E+01	1.88E+01	7.15E+00	8.75E+00	1.60E+01	4.76E+00	5.21E+00	6.58E+00	3.24E+00	3.40E+00	3.85E+00	1.80E+00	1.84E+00	2.00E+00

1.39E+01 = 1.39 × 10.

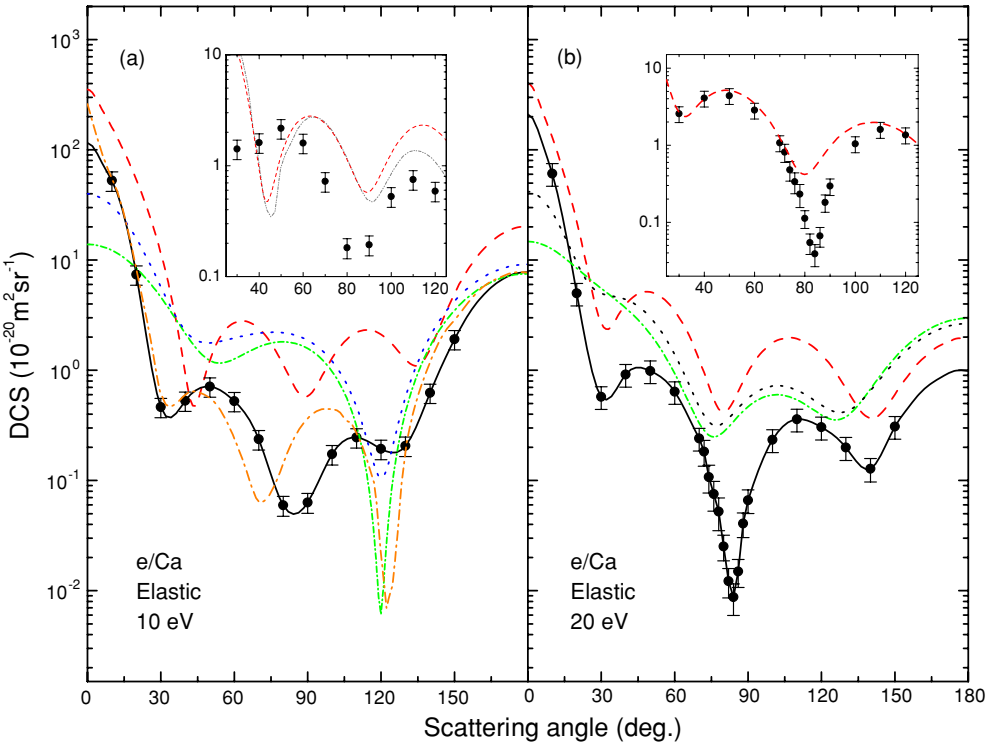

Figure 2. Differential cross sections for elastic electron scattering by Ca atom at (a) 10 eV and (b) 20 eV electron-impact energy: •, experiment; – – –, static-exchange-polarization approximation; · · ·, static-exchange approximation; -·-·-, static approximation; – · · –, SFPE, Khare *et al* [5]; – · – ·, DF, Yuan [15]. In insets, present DCSs are normalized at (a) 10° and (b) 20° on present static-exchange-polarization calculations.

DCSs, we normalized experimental results to present calculations at 20° and presented them in the inset in figure 2(b). The first and third minima coincide in position and magnitude. The second experimentally determined minimum is deeper than the theoretical and positions are shifted from one another for 4°.

Present measured and calculated data in static-exchange-polarization approximation at 40, 60 and 100 eV are shown in figure 3. Existing SFPE calculations by Khare *et al* [5] and results by Gregory and Fink [2] are also included for comparison. There is generally good agreement in shape between present calculated data and SFPE results at 40 eV (a), but our DCSs lie above SFPE calculations for $\theta < 100°$. Both minima in SFPE curve are deeper than ours. The agreement with the experiment is evident in the shape but the absolute values are higher than the experimental. The structure of the measured DCS curve at 60 eV (b) is in reasonable agreement with the theory. Both the theory and experiment obtain the inflection point at 20°, the local maximum around 100° and two minima. There is only slight displacement of these minima. For 100 eV (c) there is very good agreement between all existing calculations at all scattering angles. We have also achieved very good agreement in the shapes of angular distribution and the absolute values between experiment and theory at $\theta \leqslant 60°$. At higher angles, the agreement is not so good because calculations give generally larger cross sections and their minima are slightly shifted towards smaller scattering angles. In insets in figure 3, our experimental data normalized to the static-exchange-polarization calculation at 20° are

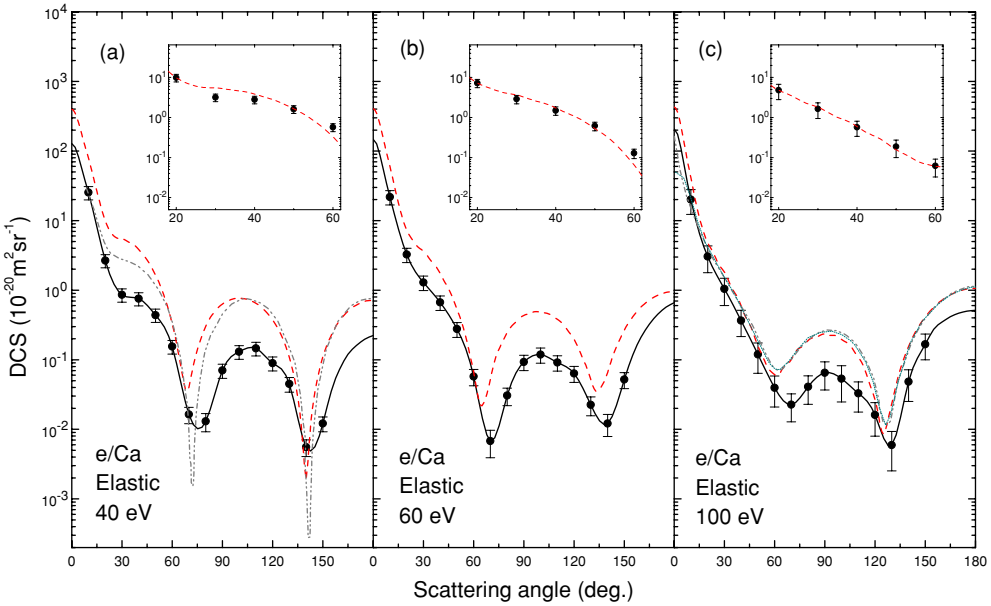

Figure 3. Differential cross sections for elastic electron scattering by Ca atom at (a) 40 eV, (b) 60 eV and (c) 100 eV electron-impact energy: •, experiment; – – –, static-exchange-polarization approximation; - - -, Gregory and Fink [2]; – · · –, SFPE, Khare *et al* [5]. In insets, present DCSs are normalized at 20° on present static-exchange-polarization calculations.

presented in the scattering angle range from 18° to 62° and they confirm the statement that there is generally good agreement in shapes of experimental and theoretical DCS curves at these higher energies.

Errors shown for the present experimental data are absolute errors. The errors were calculated as a square root of the sum of the particular squared errors and include statistical error, uncertainty of angular scale (less than 0.3°), uncertainty of energy scale (100 meV) and uncertainty of applied effective path-length correction (5%). The absolute DCSs were obtained from the intensity ratios of elastic and 4^1P^0 signal at $\theta = 10°$, so the error due to determination of the intensity ratio and normalization is included and also involve the error for the absolute DCS of the 4^1P^0 state [1]. Averaged error depends on electron-impact energy and it ranges from 20% at 10 eV to 27% at 60 eV and 40% at 100 eV.

Results of the present integral cross sections are shown in figure 4 together with available calculations since there are no other experimental Q_I results. The Q_I predicted by Khare *et al* [5] using SFPE approximation and Kelemen *et al* [16] obtained using the complex optical potentials, differ from each other and from the present experimental results at 10 eV. There are clearly significant differences in the absolute values and both theories give larger values than ours. At the same time, SFPE results [5] lie very close to our calculated results in the static-exchange-polarization approximation while SF [5] results are in better agreement with experimental and static Q_I. Static-exchange Q_I is lower than static-exchange-polarization Q_I but it is still above static and experimental Q_I. Similarly to the case for 10 eV, the static-exchange-polarization and SFPE results at 20 eV overestimate experimental data. The Q_I obtained by the static-exchange and static approximations as well as SF and results by Kelemen *et al* [16] go through the experimental integral cross section within the error bars. At 40 eV, the situation is almost the same except predicted SFPE results which decrease with energy

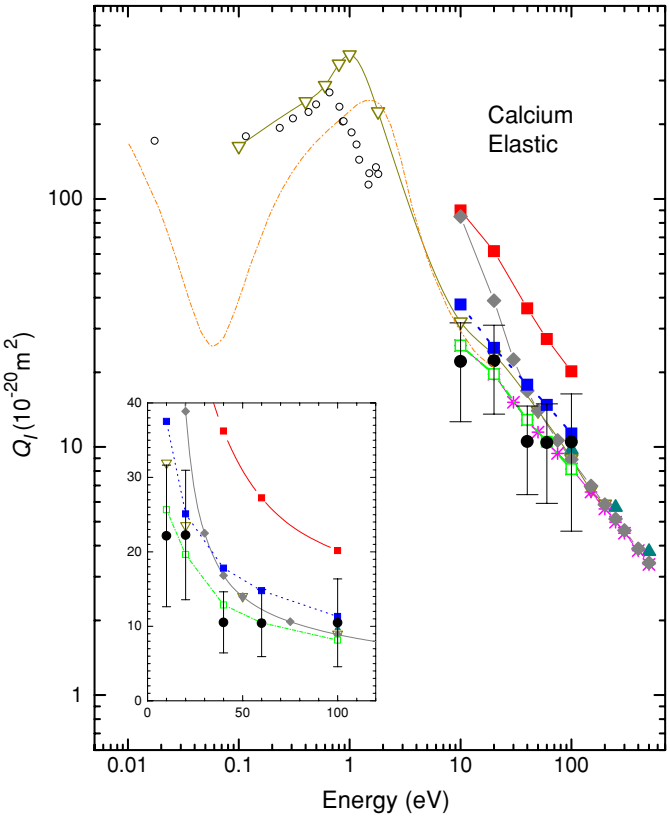

Figure 4. Integral cross sections for elastic electron scattering by Ca atom: •, present results calculated from experimental ones; —■—, static-exchange-polarization approximation; – –■– –, static-exchange approximation; –·–□–·–, static approximation; —▽—, Kelemen *et al* [16]; ▲, Gregory and Fink [2]; — ∗ —, SF, Khare *et al* [5]; —♦—, SFPE, Khare *et al* [5]; – · – ·, DF, Yuan [15]; ○, experiment, Romanyuk *et al* [3].

more rapidly than ours and corresponding Q_I is closer to the experimental. At 60 eV there are no data to compare with, while at 100 eV the experimental value is in excellent agreement with those predicted by all existing theories [2, 5, 16]. The best agreement was obtained with Q_I calculated using static approximation. The agreement is good for static-exchange approximation and it is less satisfactory with the static-exchange-polarization calculation. In figure 4, DF curve for integral cross section by Yuan [15] is also presented. From 1.4 eV to 20 eV, the general behaviour of the Q_I is similar to those by Kelemen [16] but the maximum predicted by [15] is at higher energy and its magnitude is smaller. Yuan [15] also predicts deep minimum at around 0.05 eV but unfortunately there are no other results for comparison in this region of small energies. Our experimental and static results as well as (SF) results [5] at 10 and 20 eV are in good agreement with Yuan's calculation. There is one experimental study by Romanyuk *et al* [3], which refers to the total cross section within low energy range from 0 to 10 eV. Their results obtained at energies below 1.88 eV are also included for comparison since at this energy only the elastic channel is open and total cross section is equal to the Q_I. In the plotted energy region there is one broad peak around 0.7 eV and the other smaller peak near 1.7 eV.

In comparing our experimental results to those of different authors, we find reasonable good agreement for $E_0 > 20$ eV. Our Q_I at 10 eV is relatively smaller. Possible reason for this could be the small absolute DCS of the resonant 4^1P^0 state at $\theta = 10^\circ$ which was determined through the normalization of relative DCS to the optical oscillator strength (OOS) utilizing the forward scattering function (FSF) for generalized oscillator strengths (GOS) [1]. This energy is at the limit of validity for this normalization technique, defined as 2.5 times the excitation energy.

5. Conclusions

We have investigated elastic electron scattering by calcium atom. Measurements have been performed at 10, 20, 40, 60 and 100 eV electron-impact energy and scattering angles between 10° and 150° in steps of 10° while calculation covers the same energies and the angular range of 0°–180° in 1° increments. To our best knowledge, experimental DCSs reported in this paper are the first experimental data obtained so far in this energy range. The agreement between theory and experiment was observed in the general behaviour, i.e. in both the shape and absolute value of the angular distributions of DCSs and energy dependence of integral cross sections. There is a reasonable good agreement between the experimental and calculated DCSs considering shape and this agreement is better at higher energies. The agreement considering absolute value is not so good. The static-exchange-polarization approximation gives much better agreement than static and static-exchange approximations but it is evident that adding exchange and polarization effects leads to the rising of the absolute DCS values. The absolute values obtained theoretically are generally larger than measured ones. Our calculations agree well with the other existing calculations especially at higher electron-impact energies. In comparing experimental results for integral cross sections with theoretical results, we can conclude that the best agreement was obtained with the static approximation while static-exchange-polarization calculation gives higher values. Comparison of our results with existing theoretical data shows that the agreement is good for $E_0 > 20$ eV.

Acknowledgments

This work has been carried out within project OI 1424 financed by MNZŽS of Republic Serbia. RS and RKC gratefully acknowledge the financial support from the Council of Scientific and Industrial Research (CSIR) and University Grants Commission (UGC), Delhi respectively.

References

[1] Milisavljević S, Šević D, Pejčev V, Filipović D M and Marinković B P 2004 *J. Phys. B: At. Mol. Opt. Phys.* **37** 3571
[2] Gregory D and Fink M 1974 *At. Data Nucl. Data Tables* **14** 39
[3] Romanyuk N I, Shpenik O B and Zapesochnyi I P 1980 *JETP Lett.* **32** 452
[4] Kurtz H A and Jordan K D 1981 *J. Phys. B: At. Mol. Phys.* **14** 4361
[5] Khare S P, Kumar Ashok and Vijayshri 1985 *J. Phys. B: At. Mol. Phys.* **18** 1827
[6] Amusia M Ya, Sosnivker V A, Cherepkov N A and Chernysheva L V 1985 *Sov. Phys. Tech. Phys.* **30** 1369
[7] Kazakov S M and Kristoforov O V 1985 *Sov. Phys. Tech. Phys.* **30** 476
[8] Kelemen V I, Remeta E Yu and Sabad E P 1989 *Proc. 16th Int. Conf. on Physics of Electronic and Atomic Collisions (New York)* (Amsterdam: North-Holland) Abstracts p 868
[9] Yuan J and Zhang Z 1989 *J. Phys. B: At. Mol. Opt. Phys.* **22** 2751
[10] Yuan J and Zhang Z 1990 *Phys. Rev.* A **42** 5363
[11] Gribakin G F, Gul'tsev B V, Ivanov V K and Kuchiev M Yu 1990 *J. Phys. B: At. Mol. Opt. Phys.* **23** 4505
[12] Kelemen V I, Remeta E Yu and Sabad E P 1991 *Sov. Phys. Tech. Phys.* **36** 150

[13] Gribakin G F, Gul'tsev B V, Ivanov V K, Kuchiev M Yu and Tančić A R 1992 *Phys. Lett.* A **164** 73
[14] Nikolić M R and Tančić A R 1994 *17th Summer School and Int. Symposium on the Physics of Ionized Gases (Belgrade)* ed B Marinković and Z Petrović (Yugoslavia: Institute of Physics Belgrade) Contributed papers p 14
[15] Yuan J 1995 *Phys. Rev.* A **52** 4647
[16] Kelemen V I, Remeta E Yu and Sabad E P 1995 *J. Phys. B: At. Mol. Opt. Phys.* **28** 1527
[17] Dapor M 1995 *Nucl. Instrum. Methods* B **95** 470
[18] Yuan J and Fritsche L 1997 *Phys. Rev.* A **55** 1020
[19] Remeta E Yu, Shpenik O B and Bilak Yu Yu 2001 *Tech. Phys.* **46** 375
[20] Buckman S J and Clark C W 1994 *Rev. Mod. Phys.* **66** 539
[21] Predojević B, Šević D, Pejčev V, Marinković B P and Filipović D M 2003 *J. Phys. B: At. Mol. Opt. Phys.* **36** 2371
[22] Brinkman R T and Trajmar S 1981 *J. Phys. E: Sci. Instrum.* **14** 245
[23] Joachain C J 1983 *Quantum Collision Theory* (Amsterdam: North-Holland)
[24] Srivastava R and Williamson W Jr 1989 *J. Appl. Phys.* **65** 908
[25] Clementi E and Roetti C 1974 *At. Data Nucl. Data Tables* **14** 177
[26] Furness J B and McCarthy J E 1973 *J. Phys. B: At. Mol. Phys.* **6** 2280
[27] Gianturco F A and Scialla S 1987 *J. Phys. B: At. Mol. Phys.* **20** 3171
[28] Miller T and Bederson B 1977 *Adv. At. Mol. Phys.* **13** 1
[29] Mittleman M H and Watson K N 1960 *Ann. Phys., NY* **10** 268
[30] Adibzadeh M and Theodosiou C E 2004 *Phys. Rev.* A **70** 052704